

Proceedings Article

MPI of soft ferromagnetic needles

Justin Ackers ^{a,*} · Anna C. Bakenecker ^a · Xin Chen ^b · Thorsten M. Buzug ^{a,b} ·
Matthias Graeser ^{a,b,*}

^aFraunhofer Research Institution for Individualized and Cell-Based Medical Engineering IMTE, Lübeck, Germany

^bInstitute of Medical Engineering, University of Lübeck, Lübeck, Germany

*Corresponding author, email: {justin.ackers, matthias.graeser}@imte.fraunhofer.de

© 2022 Ackers *et al.*; licensee Infinite Science Publishing GmbH

This is an Open Access article distributed under the terms of the Creative Commons Attribution License (<http://creativecommons.org/licenses/by/4.0>), which permits unrestricted use, distribution, and reproduction in any medium, provided the original work is properly cited.

Abstract

The combination of magnetic particle imaging with magnetic actuation is a promising additional application of MPI field generators aside from the imaging of SPIO tracers, because similar field configurations are needed. Since ferromagnetic materials can be manipulated easily using magnetic fields, the MPI properties of these materials are of interest to achieve a good combination of both functionalities. This work investigates the MPI signal of needle-like soft ferromagnetic objects as markers for tracking magnetic devices. Our results confirm the influence of demagnetization fields on the magnetization curve of macroscopic ferromagnetic objects and the importance of aspect ratio for the strength of the MPI signal. In addition, the spatial encoding properties of the system function are evaluated. The results show that the localization of ferromagnetic needles is possible but only in the spatial direction which is aligned with the object's long axis.

1. Introduction

The application of magnetic forces and torques under image-based supervision with magnetic particle imaging is a promising combination to enable the use of magnetically steered devices for diverse therapeutical scenarios. The applications range from the control of untethered microrobots [1] to the magnetic steering of catheters [2] and the control of magnetic nanoparticles [3].

To achieve simultaneous steering and imaging, the device needs to have the correct material properties for both functionalities. For the best MPI signal, the material ideally needs to have a step-like non-linear magnetization behavior, reaching saturation at as small as possible excitation field strengths. To respond effectively to the application of magnetic forces or torques the device needs to have a large magnetic moment, which scales directly with the volume of material used.

Due to the demagnetizing effects caused by its magnetic field, the observed magnetization curve of ferro-

magnetic materials like iron depends strongly on the object's shape and only secondarily on the actual permeability. This means for the MPI signal that soft-ferromagnetic objects of macroscopic scale with a large aspect ratio will produce an MPI signal when excited along their long axis, while more compact shapes will not. Nothnagel *et al.* observed this with needle-shaped objects and spheres made of Mu-metal [4].

For the future development of magnetic devices, these influences on the MPI signal play an important role in the design decisions involving shape and materials. Therefore, this work investigates the influence of shape and demagnetization effects on the MPI signal of soft ferromagnetic needles and evaluates the performance of ferromagnetic materials as MPI-visible markers for supervised magnetic navigation.

II. Methods and materials

To test the influence of demagnetization fields on the MPI signal of ferromagnetic objects, fine steel wool (Grade 000, mako GmbH, Germany) was chosen due to its suitable ferromagnetic properties and small diameter of individual strands. The individual strands with a diameter of about $30\ \mu\text{m}$ were cut in five different lengths from 0.5 mm to 4 mm and the magnetization response of a single strand for each length was measured in a custom magnetic particle spectrometer (MPS) with one-dimensional excitation at a sinusoidal excitation field strength of $20\ \text{mT}/\mu_0$ with a frequency of 25 kHz parallel to the long axis. The spectrum of a $10\ \mu\text{l}$ sample of undiluted Resovist (Bayer Schering GmbH, $28\ \text{mg}(\text{Fe})/\text{mL}$) was also acquired as a reference to a standard superparamagnetic MPI tracer.

To evaluate the spatial encoding properties of the needle-like objects, a 2 mm piece of the same steel wool was measured in a modified version of the 3D-spectrometer presented by Chen *et al.* [5] at excitation frequencies of $2.5\ \text{MHz}/n_i$ with $n_x = 102$, $n_y = 96$ and $n_z = 99$. The system function was measured for 41×41 offset positions with steps of $1\ \text{mT}/\mu_0$ in the xy -plane, while the sample was approximately aligned with the x -axis of the system. The signal was averaged over 100 periods to increase the SNR.

III. Results and Discussion

The results of the 1D MPS measurement are shown in Figure 1. The Resovist sample shows a comparatively steep decline in amplitude for higher frequency harmonics. In comparison, the longer steel wool samples produce harmonics at much higher frequencies due to their faster, more step-like, saturation at field strengths of only about $5\ \text{mT}/\mu_0$ as can be seen in Figure 1b.

The spectra of the steel wool samples show a dependency on the length, with the 0.5 mm sample showing a significantly steeper decline in amplitude towards higher harmonics while the difference between the samples longer than 2 mm is much smaller. This leads to the conclusion that increasing the aspect ratio above 50 results in diminishing return with respect to MPI signal strength.

Even though the material is conductive, no obvious increase in temperature could be observed through a thermal imaging camera during the measurements. However, a slight heating effect cannot be ruled out.

The results of the 3D MPS measurements are shown in Figure 2. The plot shows the signals received in the x -channel for three selected mixing frequencies, with the color's hue representing the phase and the saturation encoding the magnitude of the complex system function. The signals in the other receive channels look identical with only a scale factor in their amplitudes.

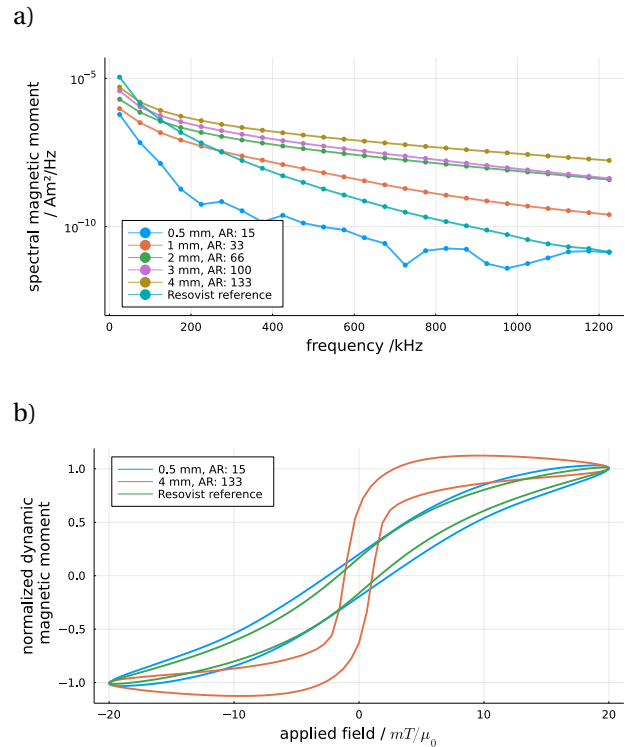


Figure 1: Measurements results of the 1D MPS measurements: a) uneven harmonics of the magnetization response, b) dynamic magnetization curve normalized to the saturation magnetization. The steel wool shows harmonics with significantly higher amplitude at higher frequencies than the Resovist reference due to the step like shape of the magnetization curve. Samples with a smaller aspect ratio produce less signal.

The pattern itself shows a banded structure tilted with an angle of four degrees from the x -axis. Since the inverse tangent of the ratio of the signal amplitudes in the x and y -channels also equals four degrees, it can be deduced that this tilt is caused by an angle between the needle axis and the x -axis of four degrees.

This structure of the system function shows what the anisotropy of the needle shape suggests: Only the orientation of the needle and the position along its axis are being encoded and can therefore be reconstructed from the received signals. Any component of the gradient field perpendicular to the needle axis does not contribute to the saturation of the object and therefore no spatial encoding perpendicular to the needle axis could be achieved.

Apart from this drawback, the strong signal at harmonics higher than 1 MHz enables the system function to encode very small differences in spatial position even exceeding the sampling rate of the measurement of $1\ \text{mT}$ which corresponds to sub-mm resolution for gradients larger than $1\ \text{T m}^{-1}$.

To achieve a complete localization of a device with ferromagnetic needles, additional spatial information

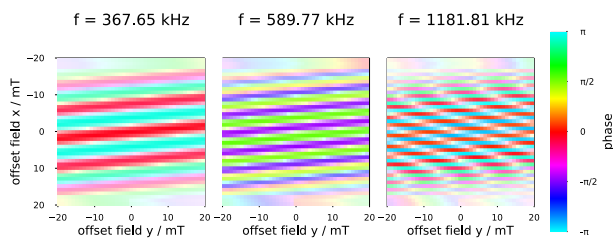


Figure 2: Selected frequencies from the complex 2D-SF for the x - y -plane on the x -channel. The hue represents the phase, while the saturation linearly encodes the absolute value of that frequency component. Each slice has been scaled to use the full saturation range. The system function shows a banded structure for all harmonics. The tilt of the bands corresponds to the tilt of the sample's long axis. The signals in the other receive channels look identical apart from a scaling factor.

needs to be encoded. This could be done by using three perpendicular needles to achieve an encoding of the position in all coordinate axes. This approach was used in the work of Nothnagel *et al.* where two needles were used to localize the object in a plane. Another alternative to using multiple needles would be the use of a thin plane of ferromagnetic materials for which the theory also predicts demagnetization fields that would allow it to produce an MPI signal and be localized inside this plane. With two intersecting planes, a full localization should be achievable.

IV. Conclusion

In conclusion, the experiments show that the use of soft ferromagnetic materials as needle-shaped markers for MPI is possible with a large SNR in the direction of the long axis but requires further consideration or design to perform a complete 3D localization.

In comparison with previous attempts to utilize iron as a marker for magnetic devices [6], the needle-shaped structures show significantly stronger MPI signal. Therefore, the next steps should include methods to incorporate the needle-shaped material into functional devices.

Combined with standard MPI tracers, the use of soft-ferromagnetic materials offers more opportunities and flexibility in the design of new and improved magnetic devices which feature clever combinations of material properties for simultaneous imaging and actuation.

However, further experiments on the imaging performance in a real selection field would be necessary as the spatial selectivity of a long needle might be different in a gradient field, where the needle is not subjected to a homogeneous field but sees a field gradient along its long axis. However, it is likely that this will not hinder the spatial resolution as the total magnetization should average out the field gradient.

Acknowledgments

Research funding: Fraunhofer IMTE is supported by the EU (EFRE) and the State Schleswig-Holstein, Germany (Project: Diagnostic and therapy methods for Individualized Medical Technology (IMTE) – Grant: 124 20 002 / LPW-E1.1.1/1536).

Author's statement

Conflict of interest: Authors state no conflict of interest.

References

- [1] A. C. Bakenecker, A. von Gladiss, H. Schwenke, A. Behrends, T. Friedrich, K. Lütke-Buzug, A. Neumann, J. Barkhausen, F. Wegner, and T. M. Buzug. Navigation of a magnetic micro-robot through a cerebral aneurysm phantom with magnetic particle imaging. *Scientific reports*, 11(1):1–12, 2021, doi:[10.1038/s41598-021-93323-4](https://doi.org/10.1038/s41598-021-93323-4).
- [2] J. Rahmer, D. Wirtz, C. Bontus, J. Borgert, and B. Gleich. Interactive magnetic catheter steering with 3-D real-time feedback using multi-color magnetic particle imaging. *IEEE transactions on medical imaging*, 36(7):1449–1456, 2017.
- [3] F. Griesse, P. Ludewig, C. Gruettner, F. Thieben, K. Müller, and T. Knopp. Quasi-simultaneous magnetic particle imaging and navigation of nanomag/synomag-d particles in bifurcation flow experiments. *International Journal on Magnetic Particle Imaging*, 6(2 Suppl 1), 2020, doi:[10.18416/IJMPI.2020.2009025](https://doi.org/10.18416/IJMPI.2020.2009025).
- [4] N. Nothnagel, J. Rahmer, B. Gleich, A. Halkola, T. M. Buzug, and J. Borgert. Steering of magnetic devices with a magnetic particle imaging system. *IEEE Transactions on Biomedical Engineering*, 63(11):2286–2293, 2016.
- [5] X. Chen, M. Graeser, A. Behrends, A. von Gladiss, and T. M. Buzug. First measurement and SNR results of a 3D magnetic particle spectrometer. *International Journal on Magnetic Particle Imaging*, 4(1), 2018, doi:[10.18416/IJMPI.2018.1810001](https://doi.org/10.18416/IJMPI.2018.1810001).
- [6] A. C. Bakenecker, A. von Gladiss, T. Friedrich, and T. M. Buzug. 3d-printing with incorporated iron particles for magnetic actuation and mpi. *International Journal on Magnetic Particle Imaging*, 6(1), 2020, doi:[10.18416/IJMPI.2020.2003001](https://doi.org/10.18416/IJMPI.2020.2003001).